Translational Oncology 13 (2020) 100865

Contents lists available at ScienceDirect

Translational Oncology

journal homepage: www.elsevier.com/locate/tranon

Original research

The association between monocytic myeloid-derived suppressor cells levels and the anti-tumor efficacy of anti-PD-1 therapy in NSCLC patients

Jiuxing Feng [a,1], Shujing Chen [b,1], Shuangqi Li [a,1], Baitong Wu [c], Jiacheng Lu [d], Li Tan [a], Jiamin Li [b], Yuanlin Song [b], Guoming Shi [d], Yujiang Geno Shi [a,e,**], Jinjun Jiang [b,*]

[a] Key Laboratory of Medical Epigenetics and Metabolism, Institutes of Biomedical Sciences, Fudan University, Shanghai 200032, China
[b] Department of Pulmonary and Critical Care Medicine, Zhongshan Hospital, Fudan University, Shanghai 200032, China
[c] School of Medicine, Tongji University, Shanghai 200120, China
[d] Liver Cancer Institute, Zhongshan Hospital, Fudan University, Shanghai 200032, China
[e] Division of Endocrinology, Diabetes and Hypertension, Brigham and Women's Hospital, Harvard Medical School, Boston, MA 02115, USA

ARTICLE INFO

Article history:
Received 29 April 2020
Received in revised form 24 July 2020
Accepted 3 August 2020

Keywords:
NSCLC
M-MDSCs
Anti-PD-1 therapy
Tregs
Immunotherapy

ABSTRACT

Monocytic myeloid-derived suppressor cells (M-MDSCs), granulocytic MDSC (G-MDSCs) and regulatory T cells (Tregs) inhibit adaptive anti-tumor immunity and undermine the efficacy of anti-PD-1 therapy. However, the impact of anti-PD-1 treatment on these immunosuppressive cells has not been clearly defined in non-small cell lung cancer (NSCLC). In this retrospective study, 27 advanced NSCLC patients were divided into partial response (PR), stable disease (SD), and progressive disease (PD) groups. The impact of anti-PD-1 therapy on circulating Tregs, G-MDSCs, and M-MDSCs was assessed by flow cytometer. Here, we found that anti-PD-1 treatment boosted circulating Tregs levels, which presented the most remarkable augment during the first two therapeutic cycles, in NSCLC patients. In contrast, anti-PD-1 therapy did not overall change G-MDSCs and M-MDSCs levels. However, the PR group had a higher baseline level of M-MDSCs, which exhibited a significant decrease after the first cycle of anti-PD-1 treatment. Besides, M-MDSCs levels in the PR group were maintained at a low level in the following therapeutic cycles. Consistently, Tregs levels robustly increased in the syngeneic tumor model after anti-mouse PD-1 Ab treatment. Accordingly, M-MDSCs neutralization by anti-mouse ly6c Ab enhanced the anti-tumor efficacy of anti-PD-1 therapy in mice. Finally, the decreased M-MDSCs levels were associated with the enhanced effector $CD8^+$ T cells expansion in the PR group and mice. In conclusion, anti-PD-1 therapy upregulates Tregs levels in NSCLC patients, and the M-MDSC levels are associated with the anti-tumor efficacy of anti-PD-1 treatment. Neutralization of M-MDSCs may be a promising option to augment anti-PD-1 therapy efficacy in NSCLC.

Introduction

The standard first-line therapy for advanced NSCLC patients consisted of platinum compounds combined with taxanes pemetrexed or gemcitabine [1]. However, these strategies only achieved approximately 26% objective response rate and the median 10 months survival [2,3]. Clinical trials have verified the effect of PD-1/L1 checkpoint inhibitors in refractory and advanced NSCLC [4–8]. In NSCLC patients, nivolumab (anti-PD-1 antibody) treatment increased the median overall survival, progression-free survival and overall survival rate compared with docetaxel chemotherapy [8]. Pembrolizumab (anti-PD-1 antibody) also have been used in advanced NSCLC patients meeting the PD-L1 cutoff point and successfully improved the overall survival up to 22.1 months [5]. However, only less than 25% of NSCLC patients met the criterion of PD-L1 expression level [9]. Unfortunately, even patients with high PD-L1 expression might be not responsive to anti-PD-L1 therapy [10]. Therefore, it's urgent to explore the pathway to resist the low efficacy and unresponsiveness to anti-PD-1 therapy in NSCLC patients.

Regulatory T cells (Tregs), defined as $CD4^+CD25^+CD127^-$ and $CD4^+CD25^+FOXP3^+$, act as an essential factor of various immune responses, including allergy, autoimmunity and immune tolerance [11,12]. Anti-PD-1immunotherapy was designed to break the immune tolerance caused by PD-1/L1 signaling pathway in $CD8^+$ T cells. However, the influence of anti-PD-1 on Tregs level has not been clearly defined. Wong et al. and Kamada et al. reported that anti-PD-1 therapy enhanced the immunosuppressive activity and survival of Tregs in F1 lupus mice and

* Correspondence to: J. Jiang, Pulmonary and Critical Care Medicine, Zhongshan Hospital, Fudan University, Shanghai 200032, China.
** Corresponding author.
E-mail addresses: Yujiang_shi@hms.harvard.edu, (Y.G. Shi), jiang.jinjun@zs-hospital.sh.cn. (J. Jiang).
[1] These authors contributed equally to this work.

http://dx.doi.org/10.1016/j.tranon.2020.100865

hyperprogressive disease (HPD) gastric patients [13,14]. In contrast, the other group reported that anti-PD-1 inhibited Foxp3$^+$ Tregs conversion in CT26 tumor-bearing mice [15]. Therefore, the impact of anti-PD-1 therapy on Tregs is remained to be studied, especially in NSCLC patients.

MDSCs, including granulocytic MDSCs (G-MDSCs, defined as CD33$^+$CD11B$^+$CD14$^-$CD15$^+$ in human and Gr-1$^+$CD11b$^+$ly6C$^-$ly6G$^+$ in mouse) and monocytic MDSCs (M-MDSCs, defined as CD33$^+$CD11B$^+$HLA-DR$^-$CD15$^-$CD14$^+$ in human and Gr-1$^+$CD11b$^+$ly6G$^-$ly6C^{hi} in mouse), exerted immunosuppressive function on T cells in cancer, autoimmune disease and viral infection [16–18]. MDSCs suppressed T cell function with multiple mechanisms, including the production of nitric oxide (NO), peroxynitrite, reactive oxygen species (ROS), and the expression of inducible nitric oxide synthase (iNOS) and arginase-1 [19,20]. G-MDSCs expressed a high level of ROS and very little NO, whereas M-MDSCs had very little ROS but a high NO level. Either increase level of ROS in G-MDSCs or NO in M-MDSCs would lead to increased peroxynitrite, which activated suppression pathways on T cells [21]. A few studies reported the association between checkpoint blockade unresponsiveness and the severe immunosuppression. For example, the myeloid cell receptor tyrosine kinases inhibitor, entinostat and SX-682, could reverse MDSCs induced immunosuppression and augment anti-PD-1 therapy in mouse models [22–24]. However, these studies did not perform further discrimination between G-MDSCs and M-MDSCs. Although G-MDSCs accounted for 80% MDSCs, another study suggested that M-MDSCs exhibited even stronger immunosuppressive function than G-MDSCs [25]. In human, studies also showed a preferential accumulation of M-MDSCs in melanoma, prostate cancer patients [26]. Also, a recent study reported the increasing CD38$^+$ M-MDSCs, rather than G-MDSCs, in metastatic colorectal cancer patients, which was targetable with an anti-CD38 monoclonal antibody [27]. Although it has been known that G-MDSCs and M-MDSCs undermined the efficacy of anti-PD-1 therapy, few associated studies investigated the impact of consecutive anti-PD-1 treatment on G-MDSCs and M-MDSCs in NSCLC patients.

Here, we demonstrated that anti-PD-1 upregulated Tregs levels, and a low M-MDSCs levels was associated with the better anti-tumor efficacy of anti-PD-1 therapy in NSCLC patients. The neutralization of M-MDSCs by ly6c mAb was associated with the expansion of effector CD8$^+$ T cells and the better anti-tumor efficacy of anti-PD-1 therapy in the mouse model.

Material and methods

Patients

Twenty-seven advanced NSCLC patients were collected from Zhongshan Hospital of Fudan University, Shanghai, China, by inclusive criterion: 1) ≥18 years old; 2) advanced NSCLC; 3) without other cancers. The peripheral blood was consecutively collected before every dosage of anti-PD-1 injection. Patients were divided into PR, PD and SD groups according to RECIST v1.1. Written informed consent forms were obtained from the patients and the study was conducted in accordance with the recognized ethical guideline and was approved by the Ethics Committee of the Institute of the Zhongshan Hospital of Fudan University. The approval number was B2019-204R.

Mice and cell line

Seven weeks old female C57BL/6 mice were purchased from LINGCHANG BIOTECH. All mice were maintained in the specific pathogen-free animal facility at Fudan University. Lewis lung carcinoma cell line was purchased from the cell bank of ATCC. All procedures about mice were approved by the Animal Ethics Committee of Fudan University.

Antibodies and reagents

All antibodies were listed below. Anti-human CD16/32 (BD catalog#564219); mouse anti-human CD3-FITC MAB HIT3A (BD catalog#555339); mouse anti-human CD11B-BB515 (BD catalog#564517); mouse anti-human CD15-APC (BD catalog#551376); mouse anti-human CD33-PE (BD catalog#555450); mouse anti-human CD14-BV605 (BD catalog#564054)□mouse anti-human HLA-DR-Percep-cy5.5 (BD catalog#552764); mouse anti-human CD45RA-PE (BD catalog#555489); mouse anti-human CD62L-BV605 (BD catalog#562719); anti-human CD25-BV421(BD catalog#564033); anti-human CD127-PE (BD catalog#557938); anti-human CCR7-Percep-cy5.5 (BD, catalog#561144); anti-human ki67-Percep-cy5.5 (BD, catalog#561284); purified rat anti-mouse CD16/32 (BD catalog#563142); rat anti-mouse CD62L-FITC (BD catalog#553150); anti-mouse CD11b-APC (Invitrogen catalog#4339583); mouse anti mouse CD45-FITC (BD catalog#553772); rat anti-mouse Gr-1 percp-cy5.5 (BD catalog#552093); rat anti-mouse Ly6c-BV421 (BD catalog#562727); rat anti-mouse CD8a-percp-cy5.5 (BD catalog#551162). rat anti-mouse CD44-PE (BD catalog#553134); hamster anti-mouse CD3e-Pacific blue (BD catalog#553066); anti-mouse CD3-BV605 (Biolegend, clone 17A2); rat anti-mouse CD4 APC-Cy7 (BD catalog#552051); anti-mouse CD25-APC (BD catalog#557192); anti-mouse CD127-BV421 (BD catalog#562959); anti-mouse iNOS-PE (Novus, Clone 4E5), anti-mouse Ki67-PE (eBioscience, Clone: SoIA15); *In vivo* anti-mouse ly6c (Bio X Cell, IgG 2a, clone MONTS-1); *In vivo* anti-mouse PD-1 (Bio X Cell, IgG 2a, clone RMP1-14); Lysing buffer 1× concentrate (BD pharmingen, catalog#555899).

Tissue processing in mouse

The peripheral blood samples of mice were collected by tail vein incision. The mice were sacrificed and the spleens, tumors and draining lymph nodes (DLN) were exteriorized. The spleens and DLN were softly homogenized by using a syringe plunger and cell strainer in cold PBS containing 2% FBS. The tumor tissue was cut into small pieces with sterile scissors and digested in PBS containing 1.5 mg/ml collagenase A and collagenase H for 3.5 h at room temperature. The tissue suspension was filtered with 70 μm cell strainer on ice to obtain single-cell suspension.

Flow cytometry

The samples were blocked with Fc block for 10 min on ice before staining procedure. For the surface staining, the cell suspension was mixed sufficiently with antibodies diluted in staining buffer and was maintained on ice in darkness for 30 min. For blood samples, we conducted staining for the whole blood. Then, 400 μl lysing buffer 1× concentrate (BD pharmingen, catalog#555899) buffer was added into 80 μl blood samples for 5 min at room temperature to remove red blood cells. The cells were collected by centrifuging at 350*g* for 5 min and were washed for two times by cold PBS. Then, we detected the percentage of targeted cells by LSR II Fortessa cytometer (BD Bioscience) after all staining procedures. Flow Jo V10 software was used to analyze the data. All procedures were performed according to the manufacturer's instructions.

Antibody therapy in human and the mouse model

In patients, the anti-PD-1 antibody was intravenously administered at 2 mg/kg for every 3 weeks (pembrolizumab, Keytruda) or 3 mg/kg for every 2 weeks (nivolumab, Opdivo) according to their therapeutic schedule. The tumor size was recorded by CT reports. The peripheral blood was collected before every dosage of anti-PD-1 injection. In mice, 1.2×10^6 logarithmic growth phage Lewis cells were subcutaneously injected on the flank of 7-weeks C57BL/6 female mice. Anti-PD-1 (200 μg/mouse/time) or anti-Ly6c (100 μg/mouse/time) were intraperitoneally injected into mice every two days post tumor injection for one week. The tumor volume was measured with a caliper and calculated with the formula: (1/2 length × width × width).

MDSCs isolation from the spleens of mice

The mice were sacrificed and the spleens were exteriorized. The spleen was softly homogenized by using a syringe plunger and cell strainer in cold PBS containing 2% FBS. The cell pellet was washed by cold PBS for two times. The cells were diluted into 1×10^8 cells/ml by suspension buffer. MDSCs were isolated according to the isolation kit protocol (stem cell, catalog#19867).

RNA extraction and RT-PCR

Total RNA was extracted from isolated MDSCs using TRIzol (Invitrogen). RNA concentrations were measured using a NANODROP 2000 (Thermo). cDNA synthesis was performed using the Prime Script RT reagent Kit with gDNA Eraser (Takara, RR047Q). Gene expression level was detected using the SYBR Premix EX Taq (Takara, RR420A) on ABI PRISM 7500 (Applied Biosystems). Gene expression level was normalized to GAPDH using the ΔC(t) method, and the results are presented as an absolute value. Gene expression level was quantified using the following primer pairs: GAPDH forward: 5′- CTAGACACCATGTGCGACGA-3′; GAPDH reverse: 5′-ATAGATGGGCACGTTGTGGG-3′; iNOS-primer 1 forward: 5′- GTTCTCAGCCCAACAATACAAGA-3′; iNOS -primer 1 reverse: 5′- GTGGACGGGTCGATGTCAC-3′; iNOS -primer 2 forward: 5′-ACATCG ACCCGTCCACAGTAT′; iNOS -primer 2 reverse: 5′- CAGAGGGGTAGGCT TGTCTC-3′. Arginase1-primer 1 forward: 5′- CTCCAAGCCAAAGTCCTTA GAG -3′; Arginase1-primer 1 reverse: 5′- GGAGCTGTCATTAGGGACATCA -3′; Arginase1-primer 2 forward: 5′- CTCCAAGCCAAAGTCCTTAGAG-3′; Arginase1-primer 2 reverse: 5′- AGGAGCTGTCATTAGGGACATC-3′.

Statistical analysis

Tests of significance between data were analyzed by using a paired (paired samples) or unpaired two-tailed (unpaired samples) student's *t*-test for single comparisons. $*P < 0.05$; $**P < 0.01$; $***P < 0.001$. A P value less than 0.05 was considered to be statistically significant. The specific statistical method was listed in the corresponding figure legend. All analysis was performed by using GraphPad Prism V7.

Results

The baseline characteristics and clinical outcomes after anti-PD-1 therapy of NSCLC patients

All patients suffered advanced NSCLC, including 21 (77.8%) IV stage, 3 (11.1%) IIB stage and 3 (11.1%) IIIB stage. The subjects consisted of 18 (66.7%) patients with adenocarcinoma and 9 (33.3%) patients with squamous carcinoma. Three (11.1%) patients had EGFR (with TKI therapy history) mutation and one (3.7%) patient had KRAS mutations. Fourteen (51.8%) patients had a history of tobacco use. Nineteen (70.4%) patients presented different extents tumor cell metastasis. The average follow-up duration was 16.9 weeks, ranging from 3.6 weeks to 38.9 weeks. Four (14.8%) patients suffered immune-related adverse events (irAEs) after anti-PD-1 therapy. Seven (25.9%) patients achieved PR and anther seven (25.9%) patients suffered PD after several cycles of anti-PD-1 therapy. Thirteen patients (48.2%) were maintained at SD status. Seven patients (25.9%) discontinued the use of anti-PD-1 therapy because of the progressive disease. Three patients (11.1%) in the PD group died after three cycles of anti-PD-1 therapy.

Anti-PD-1 therapy overall boosted the Tregs levels while showed no obvious impact on G-MDSCs and M-MDSCs levels in NSCLC patients

We analyzed the change of Tregs, G-MDSCs, and M-MDSCs before every dosage of anti-PD-1 treatment by flow cytometer (Fig. S1A–B). Compared with the baseline, anti-PD-1 therapy overall increased Treg levels after the first anti-PD-1 treatment in peripheral blood (Fig. 1A). A previous study showed that anti-PD-1 therapy decreased the frequency of M-MDSCs in NSCLC patients [28]. However, we did not observe the influence of anti-PD-1 therapy on the levels of G-MDSCs (Fig. 1B) and M-MDSCs (Fig. 1C).

Then, we wondered whether the influence of anti-PD-1 therapy on Tregs, G-MDSCs and M-MDSCs was therapeutic-cycle dependent. We found that Tregs exhibited the most remarkable increase after the first two cycles of anti-PD-1 treatment and were maintained at a high level in the following cycles (Fig. 1D). In contrast, we did not observe the significant change between the baseline levels and any post-therapy cycle in G-MDSCs (Fig. 1E) and M-MDSCs (Fig. 1F) after anti-PD-1 treatment. Collectively, anti-PD-1 therapy boosts Tregs levels in a therapeutic-cycle independent way while shows no obvious impact on G-MDSCs and M-MDSCs levels.

To exclude the influence of different anti-PD-1 antibodies, we divided patients into pembrolizumab and nivolumab groups (Table S1). Consistently, both pembrolizumab and nivolumab group obviously upregulated Tregs levels (Fig. S2A) while M-MDSCs were not changed as a whole (Fig. S2C). Noteworthily, G-MDSCs increased in nivolumab treated group but not in the pembrolizumab treated group (Fig. S2B), indicating the distinct effect of nivolumab and pembrolizumab on G-MDSCs.

Anti-PD-1 therapy upregulated Tregs in all groups of NSCLC patients while decreased M-MDSCs levels only in the PR group

To analyze the correlation between the features of the three subsets and the anti-tumor efficacy of anti-PD-1 therapy, patients were divided into PR, SD, and PD groups. We found that PR, SD and PD groups all presented a significant increase of Tregs (Fig. 2A–C). Noteworthily, Tregs in the PD group had the greatest average after the first cycle of anti-PD-1 therapy, indicating that the excessive Tregs accumulation might undermine the efficacy of anti-PD-1 therapy (Fig. S3A). Moreover, the upregulated Tregs levels are correlated with increasing Treg proliferation (Figs. 2D and S3B). In addition, we constructed the lung adenocarcinoma mouse model by subcutaneously injecting Lewis cells on the flank of seven-weeks female C57/B6 mice. To exclude the effect of tumor size, Tregs was detected two days post first time of anti-PD-1 treatment when the tumor weight is comparable between PBS and anti-PD-1 treated group (Figs. S3C and 3D). Consistently, Treg showed a significant increase in peripheral blood, DLN, spleens, and tumors after the first dosage of anti-mouse PD-1 treatment (Fig. 2E–I). The $Ki67^+$ Tregs also increased in peripheral blood and spleens after anti-PD-1 treatment in the mouse model (Fig. 2J and K). Collectively, anti-PD-1 therapy robustly promotes Tregs proliferation in NSCLC patients and the syngeneic tumor model.

Although we did not see the overall effect of anti-PD-1 therapy on G-MDSCs and M-MDSCs levels (Fig. 1B and C), we indeed observed a slight low (but failed to reach statistical significance) baseline levels of G-MDSCs in the PR group (Fig. S4A). In contrast, PR group showed a higher baseline M-MDSCs than SD and PD groups (Fig. 3A). Compared with the increased Tregs and stable G-MDSCs levels, anti-PD-1 therapy decreased the percentage of M-MDSCs specifically in the PR group (Fig. 3B) but not in SD and PD groups after the first anti-PD-1 treatment (Fig. S4B and C). Furthermore, M-MDSCs exhibited the most remarkable decrease during the first two cycles of anti-PD-1 treatment, and were maintained at a lower average level for the following therapeutic cycles compared to the baseline levels (Fig. 3C). Additionally, we also analyzed the effect of anti-PD-1 therapy on the G-MDSCs levels. However, anti-PD-1 therapy showed no significant effect on G-MDSCs in all PR, SD, and PD groups (Fig. S4D). Then, we also analyzed the distinct effect of pembrolizumab and nivolumab on the three cell populations in PR, SD and PD groups. The results showed that Tregs were obviously upregulated, especially in pembrolizumab treated PD group, and M-MDSCs still showed a significant decrease after pembrolizumab treatment in the PR group (Figs. S2D and 2F). Besides, the G-MDSCs levels were not changed (Fig. S2E). In conclusion, PR group has the specific feature of decreased M-MDSCs levels after anti-PD-1 therapy.

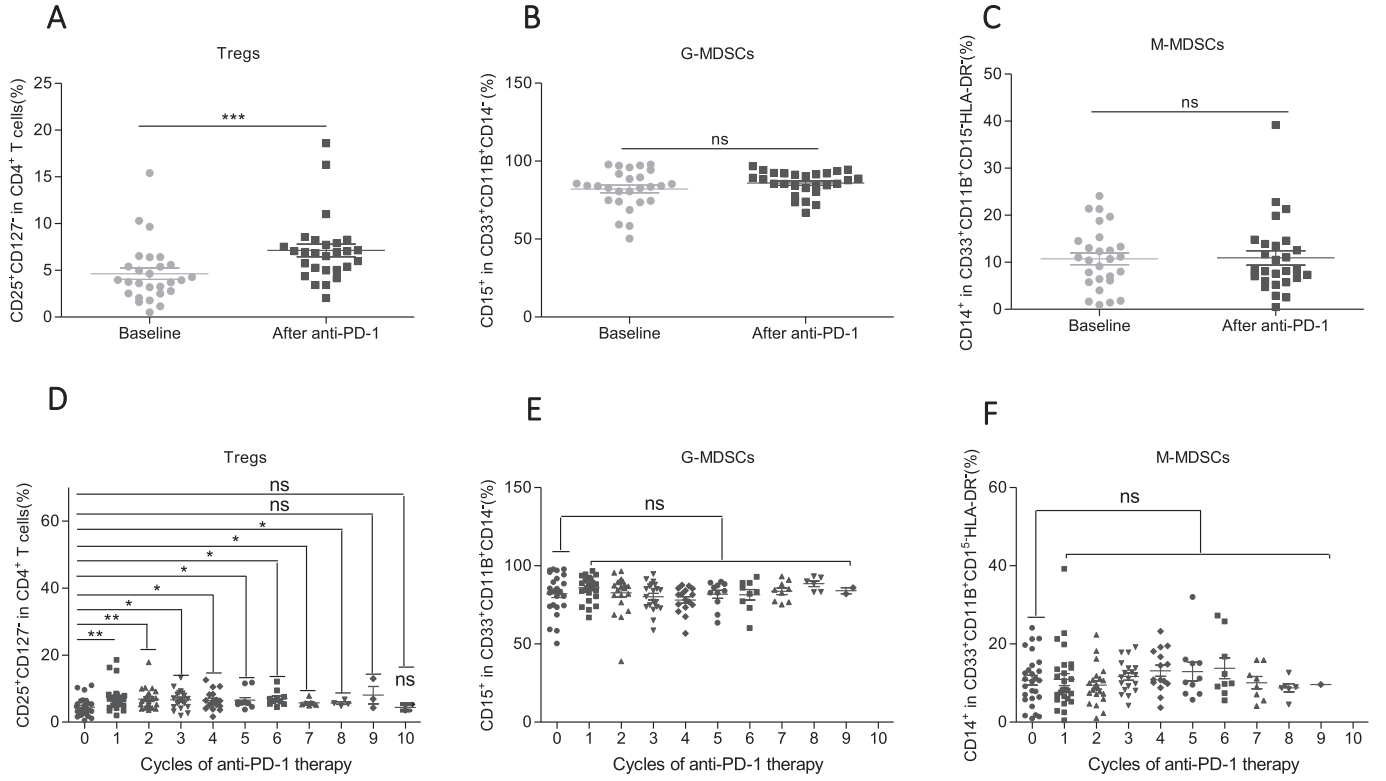

Fig. 1. Anti-PD-1 therapy overall boosted the frequency of Tregs but showed no obvious impact on M-MDSCs and G-MDSCs levels in NSCLC patients. (A–C) The overall effect of anti-PD-1 therapy on the levels of (A) Tregs, (B) G-MDSCs, and (C) M-MDSCs. "baseline" represents before PD-1 therapy; "after anti-PD-1" represents the levels after the first anti-PD-1 therapy, $N = 27$. Two-tailed paired *t*-test was performed. (D–F): The change of (D) Tregs, (E) G-MDSCs, and (F) M-MDSCs levels with consecutive dosage of anti-PD-1 therapy. X-axis: the times of anti-PD-1 treatment; Y-axis: the levels of Treg or G-MDSCs or M-MDSCs. The number of data of every cycle may be different because of the different follow-up duration of different patients. $N = 27$. Two-tailed paired *t*-test was performed between the baseline levels and any cycle of anti-PD-1 treatment. ns: no significant difference, $*p < 0.05$, $**p < 0.01$, $***p < 0.001$ compared with the control groups. A *P* value less than 0.05 was considered to be statistically significant.

To figure out whether the anti-PD-1 therapy affected the suppressive capability of MDSCs, we detected the expression of iNOS on MDSCs. The results showed that anti-PD-1 treatment did not change the levels iNOS$^+$ G-MDSCs and iNOS$^+$ M-MDSCs in peripheral blood of NSCLC patients (Figs. S4E and 4F). In the syngeneic mouse model, we also observed an obvious decrease of M-MDSCs after anti-PD-1 despite no statistical significance (Figs. S4G and 4H). Additionally, anti-PD-1 treatment did not change iNOS$^+$ G-MDSCs and iNOS$^+$ M-MDSCs in peripheral blood (Fig. S4I and J) and spleens (Fig. S4K and L) in mice. We also performed the detection of mRNA level of two immunosuppression markers, iNOS and Arginase-1, of MDSCs isolated from the spleens of PBS or anti-PD-1 treated mice. The results showed that anti-PD-1 did not significantly change iNOS and Arginase-1 mRNA levels in MDSCs (Fig. S4M). Taken together, anti-PD-1 treatment does not significantly change the suppressive capability of MDSCs.

Ly6c mAbs mediated M-MDSCs neutralization strengthened anti-tumor efficacy of anti-PD-1 therapy in mice

Considering the specific decrease of M-MDSCs in the PR group, we testified the necessity of M-MDSCs on the efficacy of anti-PD-1 therapy in inhibiting tumor growth *in vivo*. We constructed a syngeneic lung adenocarcinoma mouse model by subcutaneously injecting Lewis cells on the flank of seven-weeks female C57/B6 mice. Then, we treated the mice with PBS or anti-PD-1 or anti-ly6c or both according to the schema (Fig. 4A). Our results showed that the anti-ly6c antibody effectively neutralized almost all the M-MDSCs population in peripheral blood and spleens (Fig. 4B). We also confirmed the comparable tumor volumes among the four groups before antibody therapy (Fig. S5). Compared with the control group, anti-PD-1 and anti-ly6c only showed a very weak anti-tumor effect (Fig. 4C). In contrast, the combination of anti-PD-1 and anti-ly6c more effectively inhibited the tumor growth than either anti-PD-1 or anti-ly6c alone (Fig. 4C). The mice were sacrificed after five times of antibodies injection, and the tumor volume and weight were significantly smaller in the anti-PD-1 plus anti-ly6c group than the other three groups (Fig. 4D–F). The above results demonstrated that the neutralization of M-MDSCs enhances the response of lung adenocarcinoma mouse model to anti-PD-1 therapy.

The expansion of effector CD8$^+$ T cells are associated with the better anti-tumor efficacy in the PR group and mouse model

To further investigate the downstream executive cells for better anti-tumor effect, we performed flow cytometer analysis for the samples from multiple peripheral immune organs and tumors in mice. In mice, effector T cells were defined by CD44$^+$CD62L$^-$ (Fig. S6A). In DLN, CD8$^+$CD62L$^-$CD44$^+$ effector T cells strongly increased after anti-PD-1 plus ly6c mAbs treatment (Fig. 5A&B). In peripheral blood and spleens, we similarly observed the higher percentage of effector CD8$^+$ T cells in the anti-PD-1 plus anti-ly6c group than the control group (Fig. 5C and D). Then, we analyzed the intratumoral immune status. CD8$^+$ T cells gradually increased according to the order of PBS, anti-Ly6c, anti-PD-1 and PD-1 plus anti-ly6c groups, indicating the strongest anti-tumor effect in the anti-PD-1 plus anti-ly6c group (Fig. 5E). Importantly, the tumor-infiltrating CD8$^+$CD62L$^-$CD44$^+$ effector T cells in the anti-PD-1 plus ly6c Abs group significantly increased compared with the PBS group (Fig. 5F). Collectively, ly6c Abs mediated M-MDSCs neutralization, at least partially, enhances the anti-tumor effect of anti-PD-1 therapy by upregulating effector CD8$^+$ T cells in multiple immune organs in mice.

Next, we investigated whether the expansion of CD8$^+$ effector T cells after anti-PD-1 therapy was conserved in NSCLC patients. In human

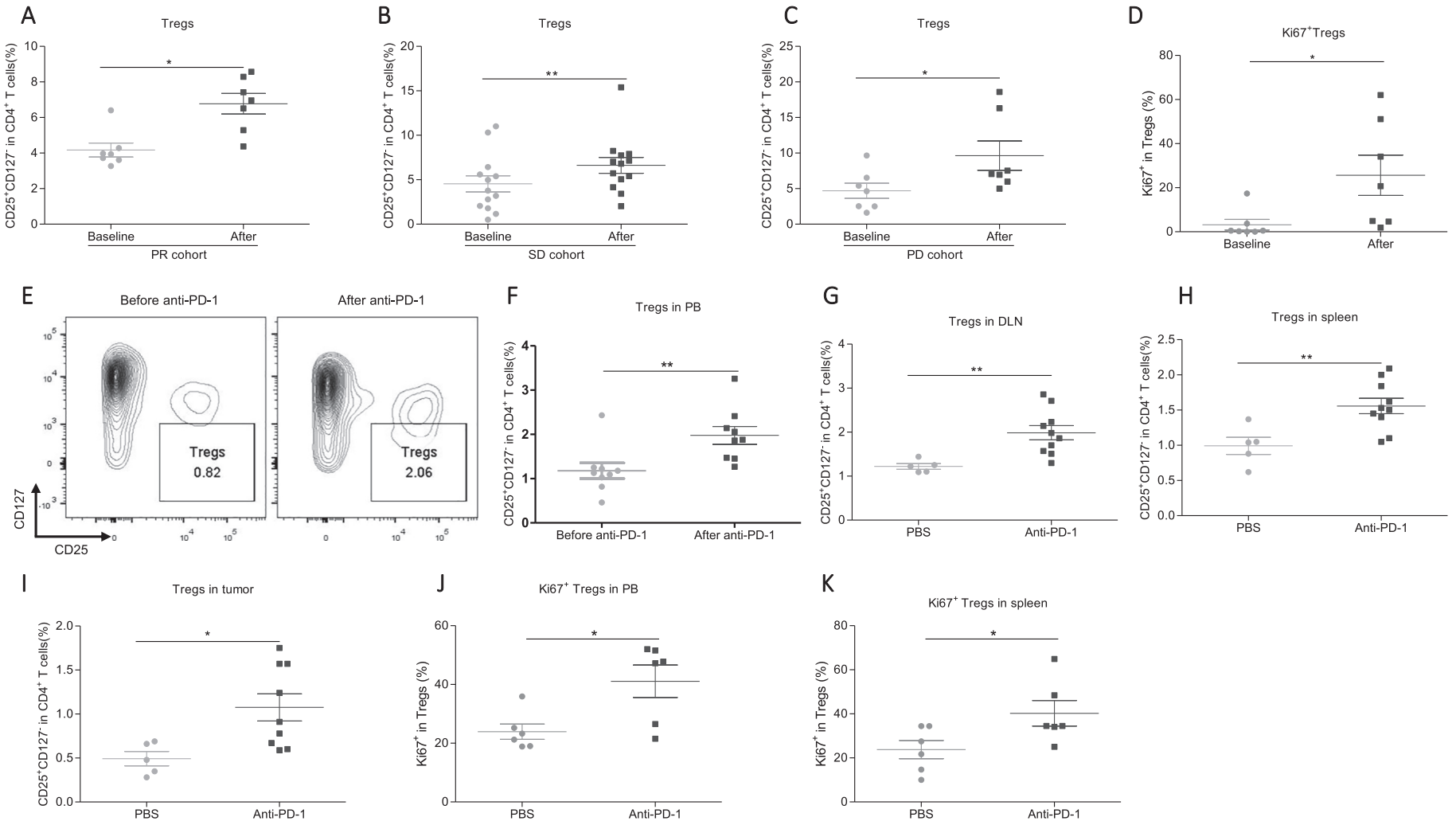

Fig. 2. Anti-PD-1 robustly upregulated Tregs levels in NSCLC patients and the syngeneic tumor mouse model. (A–C) The effect of anti-PD-1 therapy on the levels of Tregs in (A) PR, (B) SD, and (C) PD groups. PR, $N = 7$; SD, $N = 13$; PD, $N = 7$. Two-tailed paired *t*-test was performed. (D) The effect of anti-PD-1 therapy on the percentage of Ki67$^+$ Tregs in human peripheral blood. N = 7. Two- tailed paired *t*-test was performed. (E) The representative plot of Tregs of baseline and after PD-1 therapy in peripheral blood of syngeneic tumor model. (F) The effect of anti-PD-1 on the Tregs in peripheral blood of mice. Before anti-PD-1, $N = 9$; after anti-PD-1, $N = 9$. Two-tailed paired *t*-test was performed. (G–I) The effect of anti-PD-1 on the Tregs in (G) DLN, (H) spleens, and (I) tumors in mice. PBS, $N = 5$; Anti-PD-1, N = 9–10. Two tailed unpaired t-test was performed. (J–K) The effect of anti-PD-1 therapy on the percentage of Ki67$^+$ Tregs in (J) peripheral blood and (K) spleen of mice. $N = 6$. Two-tailed unpaired t-test was performed. ns: no significant difference, $*p < 0.05$, $**p < 0.01$ compared with the control group. A *P* value less than 0.05 was considered to be statistically significant.

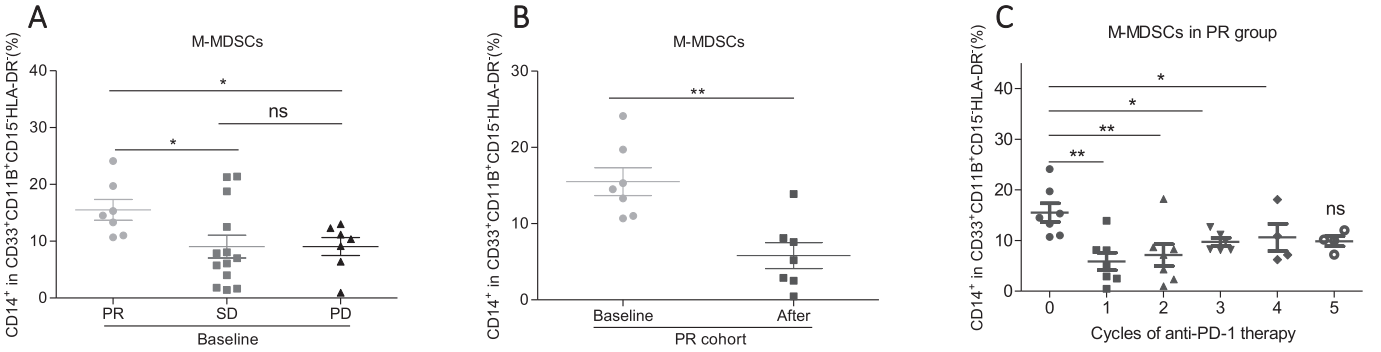

Fig. 3. M-MDSCs significantly decreased after anti-PD-1 therapy in PR group but not in SD and PD groups. (A) The baseline levels of M-MDSCs in PR, SD, and PD groups. PR, $N = 7$; SD, $N = 13$; PD, $N = 7$. Two-tailed unpaired *t*-test was performed. (B) The change of M-MDSCs levels in PR group after the first anti-PD-1 treatment, N = 7. Two-tailed paired t-test was performed. (C) The change M-MDSCs levels with a consecutive dosage of anti-PD-1 therapy. X-axis: the cycles of anti-PD-1 treatment; Y-axis: M-MDSCs frequency. The number of dots of every cycle may be different because of the different follow-up duration of different patients. N = 7. Two-tailed paired t-test was performed between the baseline levels and any cycles of anti-PD-1 treatment. ns: no significant difference, $*p < 0.05$, $**p < 0.01$ compared with the control group. A *P* value less than 0.05 was considered to be statistically significant.

samples, effector $CD8^+$ T cells were defined by $CD8^+CD45RA^+CD62L^-CCR7^-$ (Fig. S6B). Expectedly, we observed a significant increase of effector $CD8^+$ T cells in peripheral blood of PR (Fig. 5G–H) and SD (Fig. 5I) groups but not in the PD group (Fig. S6C). Additionally, the frequency of effector $CD8^+$ T cells was significantly higher in PR group compared to SD group after anti-PD-1 treatment, indicating the stronger anti-tumor response in PR group (Fig. 5J). Taken together, decreased M-MDSCs in the PR group and syngeneic mouse model may enhance anti-tumor efficacy by the expansion of effector $CD8^+$ T cells.

Discussion

It is true that the immune cell features in tumors could locally evaluate the immune status [29,30]. However, the most recent evidence convincingly demonstrated that T cells response to anti-PD-1 derived from a distinct repertoire of T cell clones that just migrated from peripheral blood [31], implying that the immune cells in peripheral blood might reflect the response of the immune system to anti-PD-1 therapy earlier. Here, we longitudinally analyzed the impact of anti-PD-1 therapy on Tregs, G-MDSCs

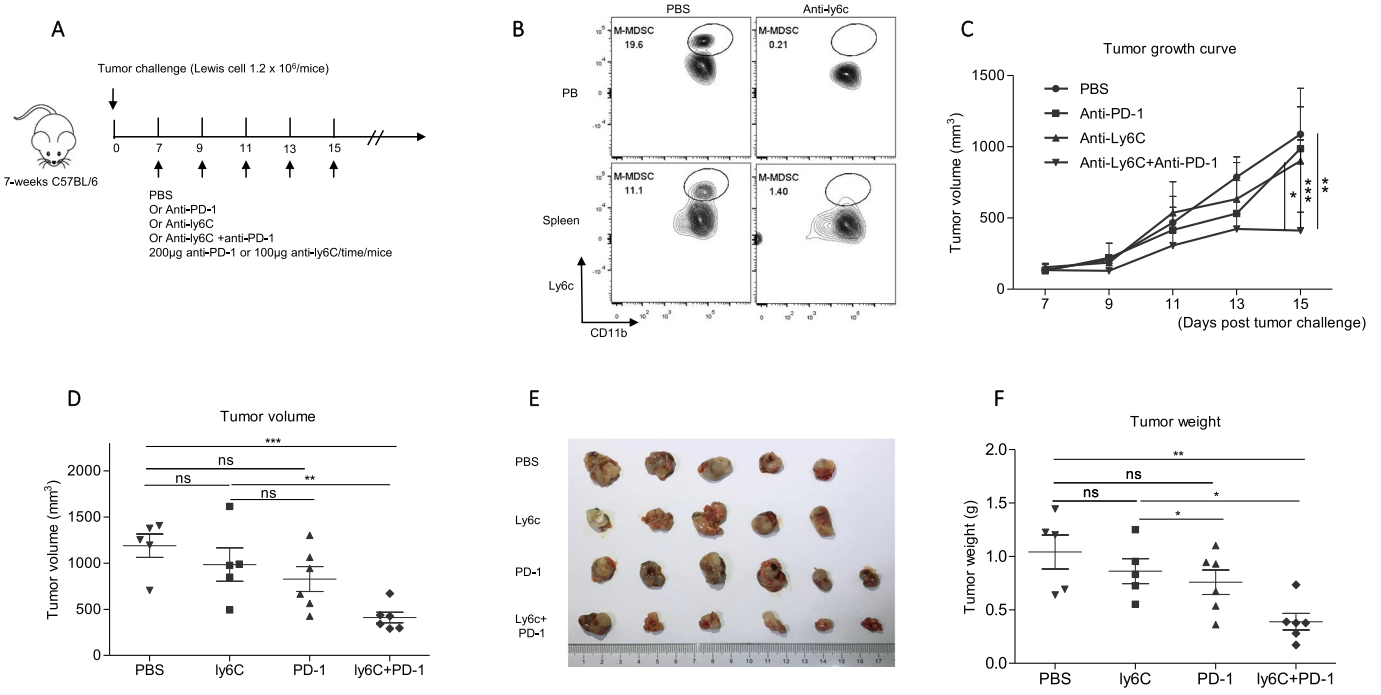

Fig. 4. Anti-mouse ly6c Abs mediated M-MDSCs neutralization promoted anti-PD-1 therapy efficacy in mice. (A) The schema to treat mice with antibodies in different groups. 1.2×10^6 Lewis lung cancer cells were subcutaneously injected into the flank of 7-weeks age C57BL/6 female mice. One week later, 200 μg anti-PD-1/time or 100 μg anti-ly6c/time or both were intraperitoneally injected mice. The mice were sacrificed after five times' treatment. (B) The frequency of M-MDSCs after anti-mouse ly6c Ab treatment in peripheral blood and spleens. The homogenized spleen single-cell suspension of the spleens and peripheral blood were analyzed by C-flow cytometry two days post ly6c treatment. The gate of M-MDSCs was $Ly6C^{hi}$ cells gated from $CD11B^+$ $Gr\text{-}1^+$ $ly6G^-$cells. (C) The tumor growth curve of different treatment groups. Two-tailed unpaired *t*-test was performed. (D) The statistics of tumor volume at the endpoint. The tumor volumes were measure by a caliper seventh days post tumor injection. PBS: $N = 5$; anti-PD-1: $N = 6$; Anti-ly6C:N = 5; Anti-PD-1 + Anti-ly6C: $N = 6$. Two tailed unpaired t-test was performed. (E) The picture of tumors at the endpoint. (F) The statistic of tumor weights at the endpoint. The tumor weights were measured by an analytical balance. Two-tailed unpaired t-test was performed. ns: no significant difference, $*p < 0.05$, $**p < 0.01$ compared with the control group. A *P* value less than 0.05 was considered to be statistically significant.

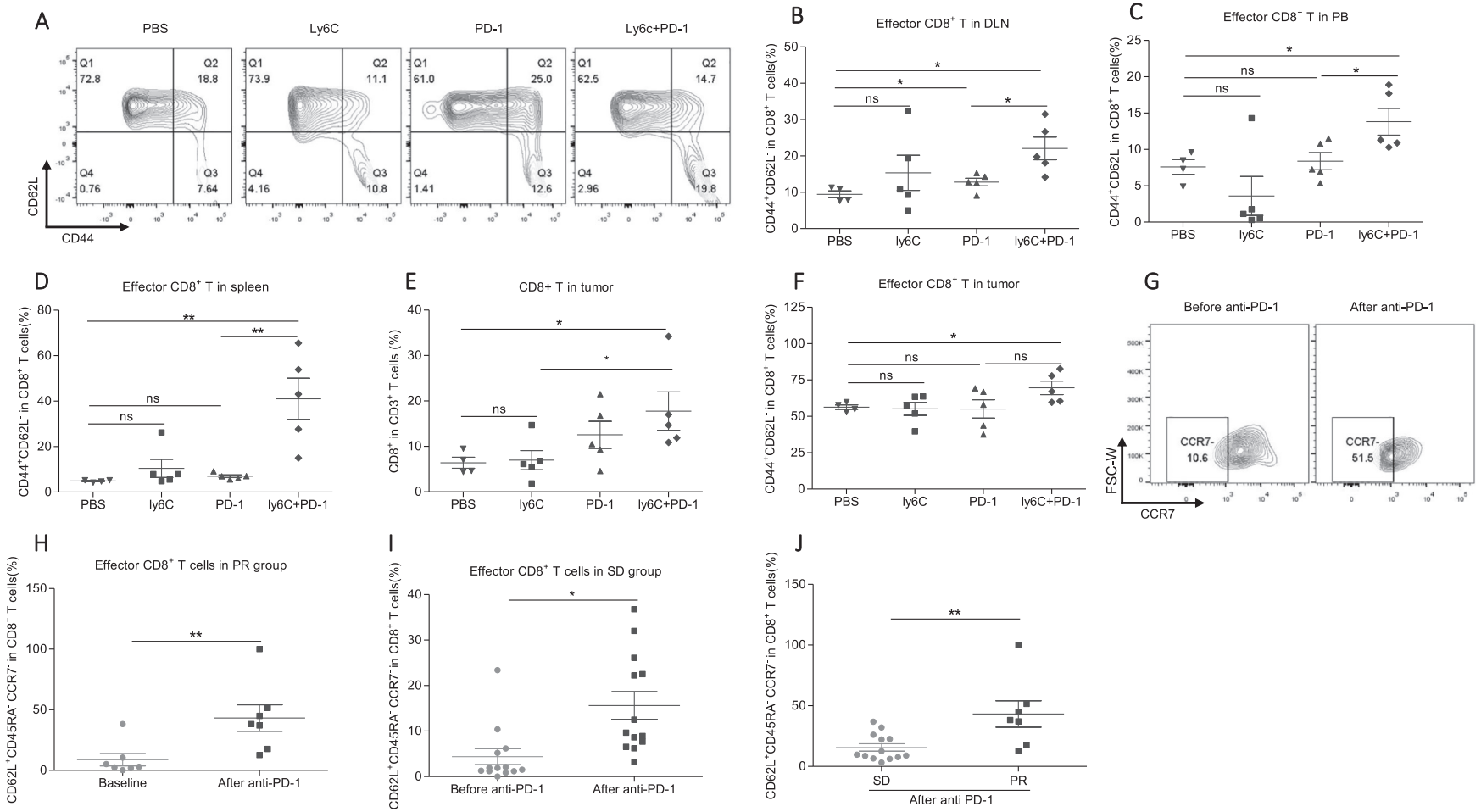

Fig. 5. The increased effector CD8$^+$ T cells are associated with the better anti-tumor efficacy in the PR group and mouse model. (A) The representative plots of CD8$^+$CD62L$^-$CD44$^+$ effector T cells in PBS (n = 4), ly6c (n = 5), PD-1 (n = 5), and ly6c + PD-1 (n = 5) groups in mice. PBS represents blank control; ly6C represents anti-ly6c therapy; PD-1 represents anti-PD-1 therapy. (B–D) The frequency of CD8$^+$CD62L$^-$CD44$^+$ effector T cells in the (B) draining lymph node (DLN), (C) peripheral blood, and (D) the spleens. PBS, n = 4; ly6C, n = 5; PD-1, n = 5; ly6C + PD-1, n = 5. Two-tailed unpaired t-test was performed. (E–F) The frequency of (E) CD8$^+$ T cells and (F) CD8$^+$CD62L$^-$CD44$^+$ T cells in tumors. PBS: N = 4; anti-PD-1: N = 5; Anti-ly6c:N = 5; Anti-PD-1 + Anti- ly6c: N = 5. Two-tailed unpaired t-test was performed. (G) The representative plots of CD8$^+$CD45RA$^+$CD62L$^-$CCR7$^-$ effector T cells in peripheral blood of the PR group. (H) The change of effector CD8$^+$ T cells in human samples after anti-PD-1 treatment in the PR group. The effector cell was defined with the panel of CD8$^+$CD62L$^-$CD45RA$^+$CCR7$^-$. N = 7. Two-tailed paired t-test was performed. (I) The effect of anti-PD-1 treatment on the level of effector CD8$^+$ T cells in the SD group. N = 13. Two-tailed paired t-test was performed. (J) The difference of effector CD8$^+$ T cells in PR and SD groups after anti-PD-1 treatment. Two-tailed unpaired t-test was performed. ns: no significant difference, *$p < 0.05$, **$p < 0.01$ compared with the control group. A P value less than 0.05 was considered to be statistically significant.

and M-MDSCs levels in peripheral blood and primarily investigated the association of M-MDSCs with the anti-tumor efficacy of anti-PD-1 therapy in NSCLC patients and the syngeneic tumor model.

Tregs are produced in the thymus as a functionally mature subpopulation of T cells and can also be induced from naive T cells in the periphery. Tregs-mediated suppression serves as a vital mechanism of negative regulation of immune-mediated inflammation and tumor inhibition [32]. However, the regulation of anti-PD-1 therapy on the Tregs is not very clear in NSCLC patients. Lydia Dyck et al. reported that anti-PD-1 inhibited $Foxp3^+$ Tregs conversion and reduced tumor-infiltrating Tregs in CT26 tumor-bearing mice [15]. On the other hand, PD-1 signaling could induce resistance to apoptosis and prolonged survival of $CD4^+$ Tregs in the F1 lupus mouse model. The blockade of PD-1 signaling by neutralizing antibody converted PD-$1^{hi}CD4^+$ Treg into PD-$1^{low}CD4^+$ Treg, which had an increased capability to promote B cell apoptosis and to suppress $CD4^+$ helper T cells [13]. In hyperprogressive disease patients of gastric cancer, the tumor-infiltrating proliferative ($ki67^+$) Tregs significantly increased after anti-PD-1 therapy. Genetic ablation or neutralizing antibody mediated blockade of PD-1 in Tregs effectively increased their proliferation and immunosuppression function [14]. The combination of Ipilimumab and anti-PD-1 also significantly elevated Tregs frequency in the spleen of CTLA4 humanized mice [33]. Consistent with the later opinion, we also detected the increased $ki67^+$ Tregs in tumor mouse model and NSCLC patients after anti-PD-1 therapy. As for the biological significance, we supposed that the upregulated Tregs on one hand might just constructively balance the excessive immune hyperfunction after anti-PD-1 therapy in NSCLC patients, which perhaps also explained the upregulating Tregs even in the PR group. On the other hand, the excessive increase of Tregs under anti-PD-1 could in turn inhibit the anti-tumor effect of anti-PD-1 therapy as shown in the PD group. Therefore, the balanced Tregs, neither too much or too less, may be crucial for the efficacy of anti-PD-1 therapy.

The distinct response of M-MDSCs to anti-PD-1 therapy may predict different anti-tumor efficacy in NSCLC patients. Recently, Laura Strauss et al. reported that PD-1 was expressed on $CD11b^+Ly6C^+$ (M-MDSCs) myeloid cells. In tumor bearing PD-$1^{f/fLysMcre}$ mice, the genetic ablation of PD-1 induced an increase of T effector memory cells with elevated antitumor function despite preserved PD-1 expression in T cells [34]. In our study, we found that the PR group had a higher level of baseline M-MDSCs than the other two groups. Therefore, we supposed that there was relatively stronger immunosuppression, at least resulting from M-MDSC, in PR group compared to SD or PD groups. Additionally, anti-PD-1 treatment could specifically decrease M-MDSCs levels in the PR group, implying that the enhanced anti-tumor efficacy in the PR group probably partially resulted from the removal of the strong immunosuppression caused by high baseline M-MDSCs. At the same time, we also observed the significant increase of effector $CD8^+$ T cells and $Ki67^+$ effector $CD8^+$ T cells (Fig. S6D) after anti-PD-1 in human and in mouse model. Taken together, the effective removal of immunosuppression and increasing proliferation of effector $CD8^+$ T cells might explain the better response to anti-PD-1 therapy in the PR group. However, the mechanism for the decreased M-MDSCs after anti-PD-1 treatment in PR group was unknown. In contrast, the SD and PD groups had relatively lower baseline levels of M-MDSCs, which might limit their response to anti-PD-1 therapy due to the less potential to release immunosuppression activity. Compared to M-MDSCs, we did not observe an obvious effect of anti-PD-1 on circulating G-MDSCs in NSCLC patients. Contrary to the high baseline M-MDSCs, we observed a slight lower baseline level of G-MDSCs in the PR group, which was not changes after anti-PD-1 treatment. Besides, G-MDSCs levels showed no change in the SD and PD groups after anti-PD-1 treatment. Therefore, the distinct response of M-MDSCs, not G-MDSCs, to anti-PD-1 therapy is associated with the anti-tumor efficacy in NSCLC patients.

Our research also has several limitations (1) the patient population is not very large (2) the patient therapy history is not exactly same (3) The lack of three cell populations features in the tumor of NSCLC patients (4) The exact mechanism for the decreased M-MDSCs after anti-PD-1 treatment was unknown in the PR group.

Conclusions

Anti-PD-1 therapy overall upregulates Tregs proliferation levels. The decreasing M-MDSCs levels are associated with the better anti-tumor efficacy of anti-PD-1 therapy in NSCLC patients. Neutralization of M-MDSCs may be a promising option to augment anti-PD-1 efficacy in NSCLC.

CRediT authorship contribution statement

Jiuxing Feng: methodology, original draft preparation, visualization. **Shujing Chen**: methodology, software, resources, funding acquisition. **Shuangqi Li**: methodology, visualization. **Baitong Wu**: formal analysis, writing-review& editing. **Jiacheng Lu**: resources. **Li Tan**: writing – Review & Editing. **Jiamin Li**: resources. **Yuanlin Song**: resources. **Guoming Shi**: software. **Yujiang Geno Shi**: supervision, project administration. **Jinjun Jiang**: conceptualization supervision, project administration, funding acquisition. All authors read and approved the manuscript prior to submission.

Declaration of competing interest

The authors declare that they have no known competing financial interests or personal relationships that could have appeared to influence the work reported in this paper.

Acknowledgements

We thank Ruijin hospital affiliated to Shanghai Jiaotong University (Jing Lu) and pathology department of Fudan University (Shuhui Sun) for their help in flow cytometry facility and data analysis. We are also thankful to all members work in the SPF mouse core at Fudan University.

Funding

This work was supported by the National Natural Science Foundation of China (grant number 81870062 and 81900038); Shanghai Top-Priority Clinical Key Disciplines Construction Project (grant number 2017ZZ02013).

Appendix A. Supplementary data

Supplementary data to this article can be found online at https://doi.org/10.1016/j.tranon.2020.100865.

References

[1] M. Mathew, T. Enzler, C.A. Shu, N.A. Rizvi, Combining chemotherapy with PD-1 blockade in NSCLC, Pharmacol. Ther. 186 (2018) 130–137.
[2] F.A. Shepherd, J. Dancey, R. Ramlau, K. Mattson, R. Gralla, M. O'Rourke, N. Levitan, L. Gressot, M. Vincent, R. Burkes, et al., Prospective randomized trial of docetaxel versus best supportive care in patients with non-small-cell lung cancer previously treated with platinum-based chemotherapy, J. Clin. Oncol. 18 (10) (2000) 2095–2103.
[3] S.G. Spiro, R.M. Rudd, R.L. Souhami, J. Brown, D.J. Fairlamb, N.H. Gower, L. Maslove, R. Milroy, V. Napp, M.K. Parmar, et al., Chemotherapy versus supportive care in advanced non-small cell lung cancer: improved survival without detriment to quality of life, Thorax 59 (10) (2004) 828–836.
[4] S. Peters, S. Gettinger, M.L. Johnson, P.A. Janne, M.C. Garassino, D. Christoph, C.K. Toh, N.A. Rizvi, J.E. Chaft, E. Carcereny Costa, et al., Phase II trial of atezolizumab as first-line or subsequent therapy for patients with programmed death-ligand 1-selected advanced non-small-cell lung cancer (BIRCH), J. Clin. Oncol. 35 (24) (2017) 2781–2789.
[5] R. Hui, E.B. Garon, J.W. Goldman, N.B. Leighl, M.D. Hellmann, A. Patnaik, L. Gandhi, J.P. Eder, M.J. Ahn, L. Horn, et al., Pembrolizumab as first-line therapy for patients with PD-L1-positive advanced non-small cell lung cancer: a phase 1 trial, Ann. Oncol. 28 (4) (2017) 874–881.
[6] R.S. Herbst, P. Baas, D.W. Kim, E. Felip, J.L. Perez-Gracia, J.Y. Han, J. Molina, J.H. Kim, C.D. Arvis, M.J. Ahn, et al., Pembrolizumab versus docetaxel for previously treated, PD-L1-positive, advanced non-small-cell lung cancer (KEYNOTE-010): a randomised controlled trial, Lancet 387 (10027) (2016) 1540–1550.
[7] A. Rittmeyer, F. Barlesi, D. Waterkamp, K. Park, F. Ciardiello, J. von Pawel, S.M. Gadgeel, T. Hida, D.M. Kowalski, M.C. Dols, et al., Atezolizumab versus docetaxel in

patients with previously treated non-small-cell lung cancer (OAK): a phase 3, open-label, multicentre randomised controlled trial, Lancet 389 (10066) (2017) 255–265.
[8] J. Brahmer, K.L. Reckamp, P. Baas, L. Crino, W.E. Eberhardt, E. Poddubskaya, S. Antonia, A. Pluzanski, E.E. Vokes, E. Holgado, et al., Nivolumab versus docetaxel in advanced squamous-cell non-small-cell lung cancer, N. Engl. J. Med. 373 (2) (2015) 123–135.
[9] M. Mathew, R.A. Safyan, C.A. Shu, PD-L1 as a biomarker in NSCLC: challenges and future directions, Ann Transl Med 5 (18) (2017) 375.
[10] A. Ribas, S. Hu-Lieskovan, What does PD-L1 positive or negative mean? J. Exp. Med. 213 (13) (2016) 2835–2840.
[11] M. Panduro, C. Benoist, D. Mathis, Tissue Tregs, Annu. Rev. Immunol. 34 (2016) 609–633.
[12] J. Saison, J. Demaret, F. Venet, C. Chidiac, C. Malcus, F. Poitevin-Later, J.C. Tardy, T. Ferry, G. Monneret, CD4 + CD25 + CD127- assessment as a surrogate phenotype for FOXP3 + regulatory T cells in HIV-1 infected viremic and aviremic subjects, Cytometry B Clin. Cytom. 84 (1) (2013) 50–54.
[13] M. Wong, A. La Cava, B.H. Hahn, Blockade of programmed death-1 in young (New Zealand Black x New Zealand White)F1 mice promotes the suppressive capacity of CD4 + regulatory T cells protecting from lupus-like disease, J. Immunol. 190 (11) (2013) 5402–5410.
[14] T. Kamada, Y. Togashi, C. Tay, D. Ha, A. Sasaki, Y. Nakamura, E. Sato, S. Fukuoka, Y. Tada, A. Tanaka, et al., PD-1(+) regulatory T cells amplified by PD-1 blockade promote hyperprogression of cancer, Proc. Natl. Acad. Sci. U. S. A. 116 (20) (2019) 9999–10008.
[15] L. Dyck, M.M. Wilk, M. Raverdeau, A. Misiak, L. Boon, K.H. Mills, Anti-PD-1 inhibits Foxp3(+) Treg cell conversion and unleashes intratumoural effector T cells thereby enhancing the efficacy of a cancer vaccine in a mouse model, Cancer Immunol. Immunother. 65 (12) (2016) 1491–1498.
[16] M. Ost, A. Singh, A. Peschel, R. Mehling, N. Rieber, D. Hartl, Myeloid-derived suppressor cells in bacterial infections, Front. Cell. Infect. Microbiol. 6 (2016) 37.
[17] D. Lai, C. Qin, Q. Shu, Myeloid-derived suppressor cells in sepsis, Biomed. Res. Int. 2014 (2014) 598654.
[18] V. Bronte, S. Brandau, S.H. Chen, M.P. Colombo, A.B. Frey, T.F. Greten, S. Mandruzzato, P.J. Murray, A. Ochoa, S. Ostrand-Rosenberg, et al., Recommendations for myeloid-derived suppressor cell nomenclature and characterization standards, Nat. Commun. 7 (2016) 12150.
[19] K. Rui, J. Tian, X. Tang, J. Ma, P. Xu, X. Tian, Y. Wang, H. Xu, L. Lu, S. Wang, Curdlan blocks the immune suppression by myeloid-derived suppressor cells and reduces tumor burden, Immunol. Res. 64 (4) (2016) 931–939.
[20] D. Alizadeh, M. Trad, N.T. Hanke, C.B. Larmonier, N. Janikashvili, B. Bonnotte, E. Katsanis, N. Larmonier, Doxorubicin eliminates myeloid-derived suppressor cells and enhances the efficacy of adoptive T-cell transfer in breast cancer, Cancer Res. 74 (1) (2014) 104–118.
[21] J.I. Youn, S. Nagaraj, M. Collazo, D.I. Gabrilovich, Subsets of myeloid-derived suppressor cells in tumor-bearing mice, J. Immunol. 181 (8) (2008) 5791–5802.
[22] A. Holtzhausen, W. Harris, E. Ubil, D.M. Hunter, J. Zhao, Y. Zhang, D. Zhang, Q. Liu, X. Wang, D.K. Graham, et al., TAM family receptor kinase inhibition reverses MDSC-mediated suppression and augments anti-PD-1 therapy in melanoma, Cancer Immunol Res 7 (10) (2019) 1672–1686.
[23] L. Sun, P.E. Clavijo, Y. Robbins, P. Patel, J. Friedman, S. Greene, R. Das, C. Silvin, C. Van Waes, L.A. Horn, et al., Inhibiting myeloid-derived suppressor cell trafficking enhances T cell immunotherapy, JCI Insight (2019) **4**(7).
[24] A. Orillion, A. Hashimoto, N. Damayanti, L. Shen, R. Adelaiye-Ogala, S. Arisa, S. Chintala, P. Ordentlich, C. Kao, B. Elzey, et al., Entinostat neutralizes myeloid-derived suppressor cells and enhances the antitumor effect of PD-1 inhibition in murine models of lung and renal cell carcinoma, Clin. Cancer Res. 23 (17) (2017) 5187–5201.
[25] L. Dolcetti, E. Peranzoni, S. Ugel, I. Marigo, A. Fernandez Gomez, C. Mesa, M. Geilich, G. Winkels, E. Traggiai, A. Casati, et al., Hierarchy of immunosuppressive strength among myeloid-derived suppressor cell subsets is determined by GM-CSF, Eur. J. Immunol. 40 (1) (2010) 22–35.
[26] S. Solito, I. Marigo, L. Pinton, V. Damuzzo, S. Mandruzzato, V. Bronte, Myeloid-derived suppressor cell heterogeneity in human cancers, Ann. N. Y. Acad. Sci. 1319 (2014) 47–65.
[27] T.A. Karakasheva, G.A. Dominguez, A. Hashimoto, E.W. Lin, C. Chiu, K. Sasser, J.W. Lee, G.L. Beatty, D.I. Gabrilovich, A.K. Rustgi, CD38 + M-MDSC expansion characterizes a subset of advanced colorectal cancer patients, JCI Insight (2018) **3**(6).
[28] A. Tzeng, C.M. Diaz-Montero, P.A. Rayman, J.S. Kim, P.G. Pavicic Jr., J.H. Finke, P.C. Barata, M. Lamenza, S. Devonshire, K. Schach, et al., Immunological correlates of response to immune checkpoint inhibitors in metastatic urothelial carcinoma, Target. Oncol. 13 (5) (2018) 599–609.
[29] S. Kurtulus, A. Madi, G. Escobar, M. Klapholz, J. Nyman, E. Christian, M. Pawlak, D. Dionne, J. Xia, O. Rozenblatt-Rosen, et al., Checkpoint blockade immunotherapy induces dynamic changes in PD-1(−)CD8(+) tumor-infiltrating T cells, Immunity 50 (1) (2019) 181–194 (e186).
[30] J.D. Fumet, C. Richard, F. Ledys, Q. Klopfenstein, P. Joubert, B. Routy, C. Truntzer, A. Gagne, M.A. Hamel, C.F. Guimaraes, et al., Prognostic and predictive role of CD8 and PD-L1 determination in lung tumor tissue of patients under anti-PD-1 therapy, Br. J. Cancer 119 (8) (2018) 950–960.
[31] K.E. Yost, A.T. Satpathy, D.K. Wells, Y. Qi, C. Wang, R. Kageyama, K.L. McNamara, J.M. Granja, K.Y. Sarin, R.A. Brown, et al., Clonal replacement of tumor-specific T cells following PD-1 blockade, Nat. Med. 25 (8) (2019) 1251–1259.
[32] A. Sharabi, M.G. Tsokos, Y. Ding, T.R. Malek, D. Klatzmann, G.C. Tsokos, Regulatory T cells in the treatment of disease, Nat. Rev. Drug Discov. 17 (11) (2018) 823–844.
[33] X. Du, M. Liu, J. Su, P. Zhang, F. Tang, P. Ye, M. Devenport, X. Wang, Y. Zhang, Y. Liu, et al., Uncoupling therapeutic from immunotherapy-related adverse effects for safer and effective anti-CTLA-4 antibodies in CTLA4 humanized mice, Cell Res. 28 (4) (2018) 433–447.
[34] S. Su, J. Zhao, Y. Xing, X. Zhang, J. Liu, Q. Ouyang, J. Chen, F. Su, Q. Liu, E. Song, Immune checkpoint inhibition overcomes ADCP-induced immunosuppression by macrophages, Cell 175 (2) (2018) 442–457 (e423).